# Superconductive behavior of quasi-one-dimensional $Nb_3Se_4$

T. Ishida,* K. Kanoda, and H. Mazaki
*Institute for Chemical Research, Kyoto University, Kyoto 606, Japan*

I. Nakada
*The Institute for Solid State Physics, The University of Tokyo, Roppongi, Minato-ku, Tokyo 113, Japan*
(Received 8 September 1983)

Superconductive behavior of $Nb_3Se_4$ has been studied in connection with a zigzag chain of Nb. We use diamagnetic supercurrents as a probe for the effect of crystalline geometry, where the actual measurements are $\chi_1' - i\chi_1''$ (a fundamental susceptibility) and $|\chi_3|$ (a third-harmonic susceptibility). $\chi_1'$ reflects the Meissner effect. In the transition curves of $\chi_1''$ and $|\chi_3|$, we observed a single peak, which is characterized by the unusual growth with the increase of measuring amplitude. We also give the simulated transition curves by means of the weakly coupled chain model. It is interpreted that the amplitude-dependent growth of the peak is due to a disorder in the weak couplings.

## I. INTRODUCTION

Reduced dimensionality in superconductors brings various interesting properties. Lower-dimensional superconductors are considered as three-dimensional (3D) materials made of lower-dimensional inclusions bonded by Josephson junctions. For example, the Chevrel compounds[1] may be regarded as an aggregate of zero-dimensional (0D) superconducting clusters. A bundle of one-dimensional (1D) fibers appears in $(SN)_x$ (Ref. 2) and artificial, proximity-coupled Nb-Ti fibers.[3,4] The 1D nature of transition-metal chalcogenides $MX_3$ (Ref. 5) and $Nb_3X_4$ (Ref. 6) is originated by microscopic metallic chains. The layered compound $TaS_2$-(pyridine) (Ref. 7) can be viewed as a stack of very thin films. These systems may show a two-step superconducting transition.[8] One is the transition of individual inclusions (the phase-disorder transition). The other is the phase-coherent transition over the system, which is achieved by the Josephson interaction between inclusions.

When the magnetic field is applied upon a superconductor in the temperature region of the second transition, the motion of flux quanta is restricted by the vortex current circulating through the Josephson junctions involved. It is therefore meaningful to see the magnetic response of a superconductor for examining the microscopic networks in a lower-dimensional superconductor. In our previous works[4,9,10] we proposed employing a third-harmonic susceptibility $|\chi_3|$ as a probe for the second transition. The magnetic approach was also attempted by Deutscher *et al.*[11] in studying the topology of superconducting micronetworks. With artificial proximity-coupled Nb-Ti fibers,[3,4] the existence of two superconducting transitions at ~8.5 and ~2 K was confirmed by means of diamagnetic susceptibility. The 8.5-K transition was caused by individual Nb-Ti fibers. The parameter $|\chi_3|$ was sensitive only to the 2-K transition.

$Nb_3Se_4$ manifests a quasi-1D property, which directly comes from a zigzag chain running along the *c* axis of the hexagonal crystal.[12–14] Experimentally, when the inclusions are too small to detect the first transition by means of volume effect, or two transitions are adjacent, the transition of lower-dimensional superconductors occurs outwardly in one step. The unusual magnetic behavior of $(SN)_x$ was investigated by Oda *et al.*[15] and Bastuscheck *et al.*[16] Since they referred to the susceptibility as an effective property of a flux-quanta motion, the higher-harmonic process was not discussed. In the present study we apply the $|\chi_3|$ method to a synthetic 1D material for the first time. A brief account of the present work has been previously reported.[17]

## II. EXPERIMENTAL

### A. Sample preparation

The samples are prepared by the chemical vapor deposition method, where iodine is used as a transport agent.[18] The starting material is a pressed pellet of sintered polycrystalline $Nb_3Se_4$ powders. The purity of Nb is 99.9% and Se is 99.9999%. The pellet is set at the center of a quartz ampoule (1.5 cm in diameter and 15 cm in length) together with the transport agent. After evacuation ($5\times10^{-4}$ Torr), the ampoule is sealed and is placed in the middle of a horizontal electric furnace. Temperature is kept at 1000 °C, of which the temperature gradient is 3 °C/cm along the axis. After a few weeks, tiny needlelike single crystals grow from the pellet towards the higher temperature region.

The grown crystals were examined by the x-ray powder diffraction analysis and identified to be $Nb_3Se_4$ with hexagonal structure, which is consistent with other reports.[12,13] The whiskers grow always along the crystallographic *c* axis. This was confirmed with the x-ray oscillation photography.

These crystals were loosely assembled along their *c* axes and glued together with GE7031 varnish for adhesion and electrical insulation between single crystals. Then, the sample was cut in a rectangular shape (50–100 mg of $Nb_3Se_4$).

 

### B. Measuring system

The fundamental ac susceptibility $\chi_1' - i\chi_1''$ is measured by using a two-phase lock-in analyzer (Ithaco model 393). The null adjust of the bridge is made at temperature slightly above the superconducting transition. The phase of the lock-in analyzer is set to give variation only to the in-phase signal but not to the out-of-phase signal, when the variable standard mutual inductance (Tinsley model 4229) of the bridge is altered. This setting was confirmed not to be affected by the change in coil temperature from 4.2 K down to 1.3 K.[19] The null adjust and phase setting are repeated in each measurement.

In the measurement of $|\chi_3|$, the lock-in analyzer locks to an external reference frequency, which is 3 times the exciting frequency $f$. The amplitude of signal is deduced from the vector summer of the lock-in analyzer by using in-phase and out-of-phase signals. $|\chi_3|$ can be measured as an amplitude of the third-harmonic component in off-balance signal of the bridge, being usually very small. We paid careful attention to adjusting zero points of in-phase and out-of-phase signals to get the precise vector sum.

The sample is mounted in a Lucite holder to fix the direction of magnetic field to the $c$ axes. Then the sample is directly immersed in a liquid-helium bath. Calibrations of the Ge thermometer located near the sample were made with respect to a helium vapor pressure. We developed an approximate relation between a Ge resistance $R$ and a corresponding temperature $T$ as

$$\log_{10}T = \sum_{i=1}^{13} c_i(\ln R/100)^{i-1} . \qquad (1)$$

This formula is convenient compared to a relation[20]

$$\ln R = \sum_{i=1}^{N} a_i(\ln T)^{i-1} , \qquad (2)$$

because one can directly calculate a temperature from the measured resistance. With the calibrated points, we performed the least-square fit to Eq. (1). The uncertainty of the thermometer was estimated to be $\pm 10$ mK in absolute value and the resolution was better than 0.1 mK. The voltage drop of the thermometer is fed into a digital voltmeter with the resolution of 0.1 $\mu$V (Takeda model TR6877). The voltmeter is controlled by a microcomputer (Hewlett-Packard model HP-85). Thus we can immediately find the temperature.

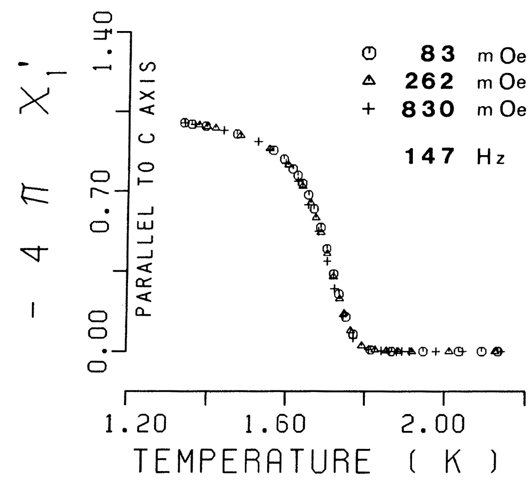


FIG. 2. $\chi_1'$ vs $T$. The ac magnetic field is applied parallel to $c$ axis of $Nb_3Se_4$.

## III. RESULTS AND DISCUSSION

### A. Fundamental susceptibility

Superconductive $Nb_3Se_4$ may respond in a nonlinear manner against an external ac magnetic field. In the present study we observed the response at two different frequency channels. One is at a fundamental frequency $f$, and the other is at a third-harmonic frequency $3f$.

The ac fundamental susceptibility was measured with respect to temperature $T$ as well as to the amplitude of external magnetic field $h_0$. In Fig. 1 are shown the typical results of real-part susceptibilities $\chi_1'$, where the magnetic

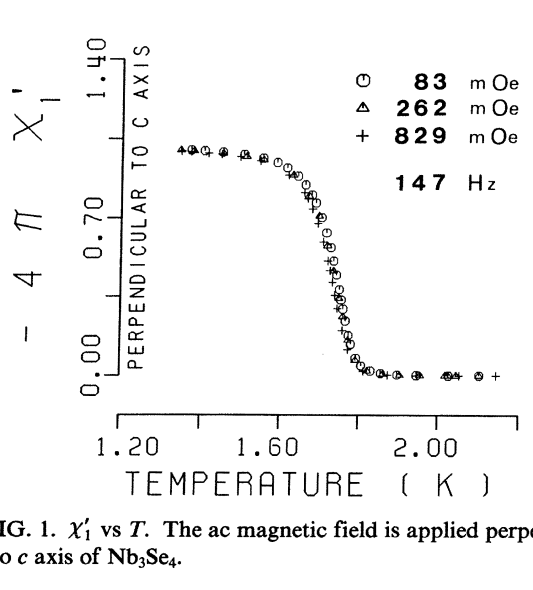


FIG. 1. $\chi_1'$ vs $T$. The ac magnetic field is applied perpendicular to $c$ axis of $Nb_3Se_4$.

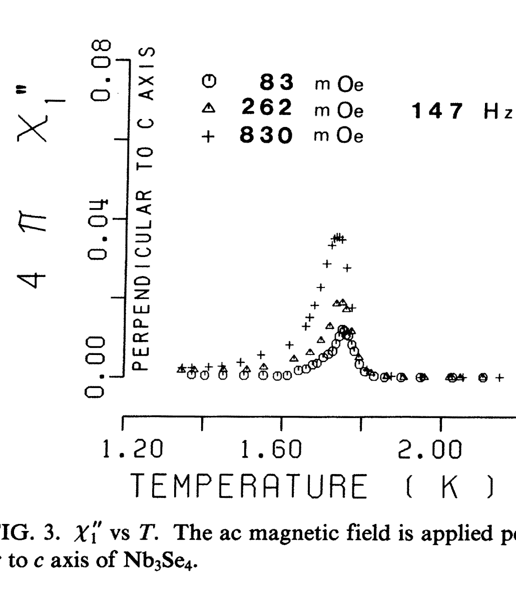


FIG. 3. $\chi_1''$ vs $T$. The ac magnetic field is applied perpendicular to $c$ axis of $Nb_3Se_4$.

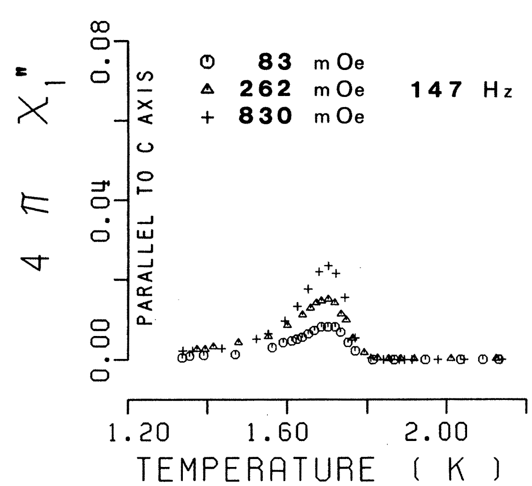


FIG. 4. $\chi_1''$ vs $T$. The ac magnetic field is applied parallel to $c$ axis of $Nb_3Se_4$.

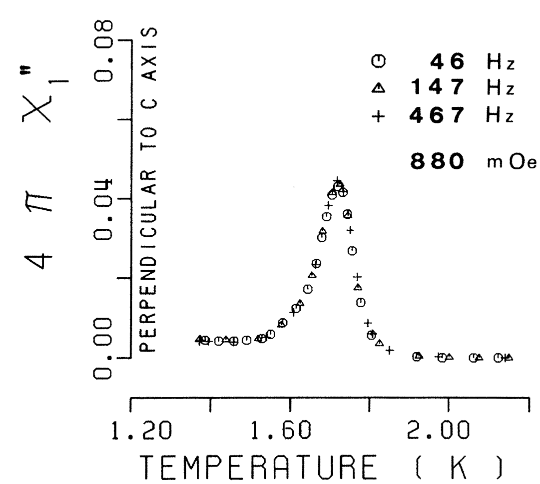


FIG. 6. Frequency dependence of $\chi_1''$ in superconducting transition of $Nb_3Se_4$.

field ($f=147$ Hz) was applied perpendicular to $c$ axis. Figure 2 shows $\chi_1'$ obtained with the field parallel to the $c$ axis. In both figures, the vertical scales are normalized to the $\chi_1'$ value taken at the lowest $T$ and at the smallest $h_0$. Clearly, the Meissner effect appears. In Figs. 3 and 4 the $\chi_1''$ transition curves are shown for fields perpendicular to and parallel to the $c$ axis, respectively. $\chi_1''$ forms a peak during the transition. This peak grows with the increase in $h_0$. When $h_0$ is small, the transition curve is not smooth. At lower temperatures, $\chi_1''$ has the tail.

There are noticeable differences between the two cases (perpendicular and parallel field). (a) The Meissner effect is more clearly brought out in Fig. 1 than in Fig. 2. $\chi_1'$ in Fig. 1 saturates at temperatures lower than 1.5 K, but $\chi_1'$ in Fig. 2 gradually increases even at lower temperatures. (b) When $h_0$ increases, the transition curve shifts, but the extent of diamagnetism is not altered at the lowest temperature. The transition curves in Fig. 2 are less dependent on $h_0$ compared to those in Fig. 1. (c) The peak formation is more evident in the perpendicular field (Fig. 3) than in the parallel field (Fig. 4). (d) Compared to the transition curves in the parallel field, those in the perpendicular are sharper but more sensitive to $h_0$. Note that similar differences were also reported in fibrous $(SN)_x$.[15]

It is well known that an appearance of $\chi_1''$ means a dissipative state of sample. There are some cases where the dissipation is caused by the frequency-dependent mechanism, such as eddy current loss. So, we examined the dependence of ac susceptibility with another $Nb_3Se_4$ sample. The results shown in Figs. 5 and 6 do not give an appreciable difference for three different frequencies: 46, 147, and 467 Hz. Thus the $\chi_1'$ and $\chi_1''$ profiles shown in Figs. 3 and 4 rule out the possibility of employing an effective conductivity model.[21]

### B. Third-harmonic susceptibility

Diamagnetic shielding currents play a more prominent role in $|\chi_3|$ than in $\chi_1$. The $|\chi_3|$ measurements were

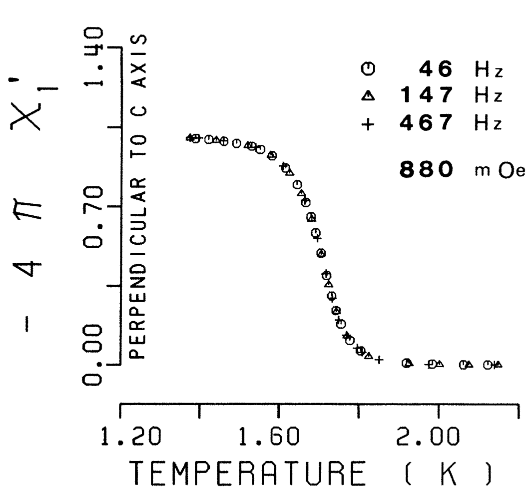


FIG. 5. Frequency dependence of $\chi_1'$ in superconducting transition of $Nb_3Se_4$.

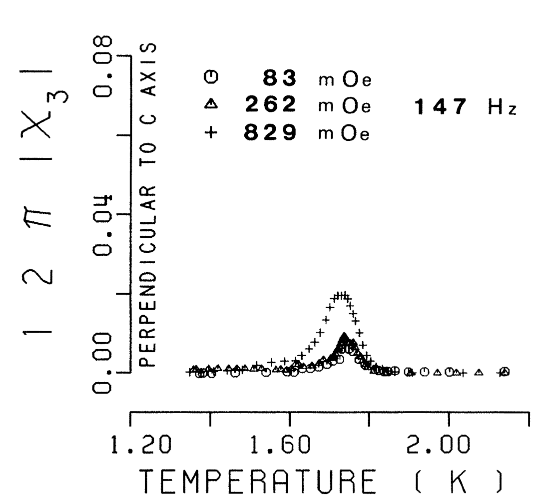


FIG. 7. $|\chi_3|$ vs $T$. The ac magnetic field is applied perpendicular to $c$ axis of $Nb_3Se_4$.

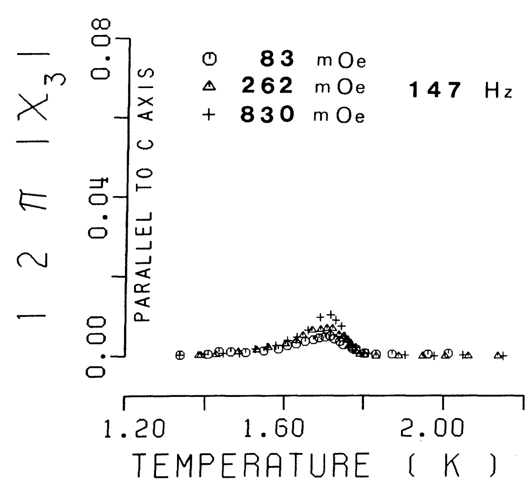


FIG. 8. $|\chi_3|$ vs $T$. The ac magnetic field is applied parallel to $c$ axis of $Nb_3Se_4$.

performed with respect to $T$ as well as $h_0$. In Figs. 7 and 8 we show, respectively, the transition curves of $Nb_3Se_4$ in terms of $|\chi_3|$ in the fields perpendicular to and parallel to the $c$ axis. In Fig. 7 the $|\chi_3|$ curves at 83 and 262 mOe are not smooth with respect to $T$. Good reproducibility indicates that this is not due to an experimental error. When $h_0$ increases up to 829 mOe, the $|\chi_3|$ curve grows and changes smoothly over the wider temperature region. In the case of the parallel field (see Fig. 8) the $|\chi_3|$ behavior is very similar to the perpendicular field. However, the peak height is appreciably lower than that of Fig. 7. Comparing the $|\chi_3|$ curve (Figs. 7 and 8) with the $\chi_1''$ curve (Figs. 3 and 4), one can acknowledge the close similarity, except the peak positions and heights. Since $|\chi_3|$ does not appear in an ordinary superconductor, the present results could be related to the 1D crystalline morphology of $Nb_3Se_4$.

### C. Weakly coupled chain model

The crystal structure of $Nb_3Se_4$ is characterized by the Nb chains running along the $c$ axis. The distance between the Nb atoms in a chain is metallic, but the interchain distance exceeds the metallic distance. This is the structural origin of quasi-1D nature. It is useful to model the specimen as an aggregate of 1D chains that are weakly coupled through the Josephson-type junctions.

In Fig. 9 we approximate the specimen by a $10\times10$ mesh of randomly coupled chains. In the figure, the vertical bars correspond to the zigzag chains and the horizontal symbols represent the Josephson junction. Here, we suppose that the direction of applied magnetic field is perpendicular to the $c$ axis. The coupling strength is considered to be slightly randomized within the system. The sources of randomness are (1) the superconducting fluctuation effect in the 1D system, (2) the grain size, (3) the crystal imperfection such as dislocation, (4) the junction resistance, (5) the electronic mean free path, and (6) the proximity effect. We take these effects into consideration in terms of distribution in the transition temperatures and the Josephson critical currents.

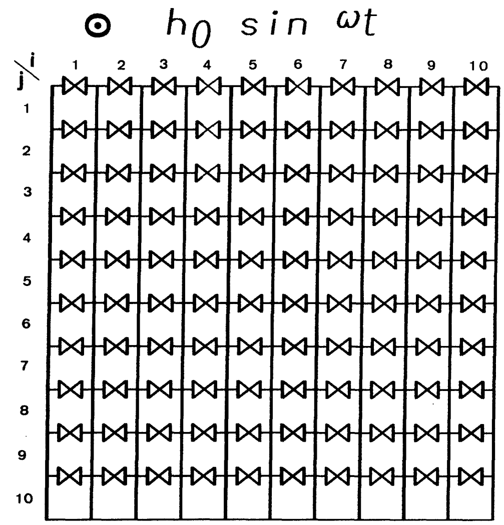


FIG. 9. Schematic diagram of the weakly coupled chain model. The field is applied perpendicular to $c$ axis. The vertical lines represent the Nb chains and the horizontal symbols represent the weak coupling between the chains.

In regard to the magnetic behavior of $(SN)_x$, two different interpretations were reported.[15,16] One is based on the tunneling junction between $(SN)_x$ fibers, and the other is based on the proximity junction. This indicates that the interaction type is still controversial.

Here we attempt to find the overall picture of the randomly coupled 1D system on the basis of the tunnel-type coupling. For a tunnel junction, the critical current density at temperature $T$ is given by

$$J(T)=\frac{\pi\Delta(T)}{2eR}\tanh\frac{\Delta(T)}{2kT} \ . \tag{3}$$

At temperatures near $T_0$, $J(T)$ shows a linear temperature dependence. In the following discussion we restrict the temperature region to the vicinity of superconducting transition. We assign the critical current of the Josephson junction located at the upside of region $(i,j)$ by

$$J_{i,j}(T)=\begin{cases} J_0 g_{i,j}(1-T/f_{i,j}T_0), & T<f_{i,j}T_0 \quad (4)\\ 0, & T\geq f_{i,j}T_0 \ . \quad (5)\end{cases}$$

Here $f_{i,j}$ and $g_{i,j}$ are the independent parameters representing the distribution in the transition temperatures and the critical currents at $T=0$. For all sets of $(i,j)$, $f_{i,j}$ and $g_{i,j}$ form a Gaussian distribution of a mean value 1.0 and a standard deviation 0.1.

When an external sinusoidal magnetic field $h(t)$ is imposed upon the network, the magnetic field begins to enter the network through the junctions. In the region $(i,j)$ the magnetic field at time $t_k$ is expressed by $b_{i,j}(t_k)$, which is set to zero at $t_k=0$ (the initial state). We sequentially generate $h(t_k)=h_0\sin(2\pi f t_k)$ for $k=1-128$, where $t_k=(k-1)/128f$. We define $b_{i,0}(t_k)$ as equal to $h(t_k)$. For each row $(i)$, the magnetic field enters the network step by step. We examine the magnetic field difference $D_{i,j}(t_k)$ between neighboring regions separated by the junction $(i,j)$, where $D_{i,j}(t_k)=b_{i,j}(t_{k-1})-b_{i,j-1}(t_k)$. The relation between $D_{i,j}(t_k)$ and $J_{i,j}(T)$ reduces to three cases. Then, the magnetic field $b_{i,j}(t_k)$ can be determined by the following criteria:

$$b_{i,j}(t_k)=\begin{cases} b_{i,j}(t_{k-1}), & |D_{i,j}(t_k)| \leq 4\pi J_{i,j}(T)/c & (6) \\ b_{i,j-1}(t_k)+4\pi J_{i,j}(T)/c, & D_{i,j}(t_k) > 4\pi J_{i,j}(T)/c & (7) \\ b_{i,j-1}(t_k)-4\pi J_{i,j}(T)/c, & D_{i,j}(t_k) < -4\pi J_{i,j}(T)/c \;. & (8) \end{cases}$$

Thus we can determine $b_{i,j}(t_k)$ in a manner that enables the shielding of $D_{i,j}(t_k)$ by the Josephson diamagnetic current $J_{i,j}(T)$. The procedure is executed for all regions ($i=1$—$10$, $j=1$—$10$). The magnetic field $B(t_k)$ is evaluated by averaging the local magnetic fields as

$$B(t_k)=\sum_{i,j} b_{i,j}(t_k)S_{i,j} \Big/ \sum_{i,j} S_{i,j} \;, \qquad (9)$$

where $S_{i,j}$ is a cross-sectional area of region $(i,j)$ and the area is assumed to be the same for all regions. This process is repeated for another period of ac magnetic field to find a stationary behavior. The generated $B(t)$ is transformed into the magnetization $M(t)$. The Fourier expansion of $M(t)$ is expressed by

$$M(t)=\sum_{n=1}^{\infty} h_0[\chi_n'\sin(2\pi nft)+\chi_n''\cos(2\pi nft)] \;. \qquad (10)$$

From this expression, $\chi_1'$, $\chi_1''$, and $|\chi_3|=(\chi_3'^2+\chi_3''^2)^{1/2}$ are estimated by the Fourier analysis at 51 points of temperature. We carried out these calculations by using five different relative values of $h_0$ (90, 50, 30, 10, and 5), while $J_0$ is kept constant. As shown in Fig. 10, we get the transition curves of $\chi_1'$, $\chi_1''$, and $|\chi_3|$, where the temperature scale is arbitrary.

From the simulated curves of Fig. 10, one can see the following superconductive behaviors. (a) $\chi_1'$ reflects the Meissner effect and the curve shifts toward lower temperatures as $h_0$ increases. (b) The peak of $\chi_1''$ grows with the increase in $h_0$. (c) When $h_0$ is small, the calculated points of $\chi_1''$ are rather scattered. The $\chi_1''$ curve becomes smooth at higher amplitudes and has the tail at lower temperatures. (d) The behavior of $|\chi_3|$ is very similar to that of $\chi_1''$. (e) The temperature corresponding to the top of the peak is not the same in $\chi_1''$ and $|\chi_3|$. The items (a)—(e) explain well the observed profiles of $\chi_1'$, $\chi_1''$, and $|\chi_3|$ of $Nb_3Se_4$. We have also performed the model calculations with $20\times20$, $30\times30$, and $40\times40$ networks. Results are essentially the same as the $10\times10$ case. Since we have not specified frequency in the calculation, the curves in Fig. 10 are naturally frequency independent. This is consistent with the experimental results (see Figs. 5 and 6). We emphasize that the drastic peak growth of $\chi_1''$ and $|\chi_3|$ could not be reproduced without considering randomizing parameters $f_{i,j}$ and $g_{i,j}$. The unusual behavior of ac response among various lower-dimensional superconductors is considered to be connected with the crystalline geometry, and the response of superconducting micronetworks is effectively characterized by the appearance of $|\chi_3|$. In particular a weak randomness of couplings between inclusions is responsible for the amplitude-dependent growth of the $\chi_1''$ and $|\chi_3|$ peaks.

The present calculation is focused upon the cases where the crystalline $c$ axis is perpendicular to the direction of magnetic field. In the case of parallel field, the diamagnetic currents are circulating in a percolating network. It

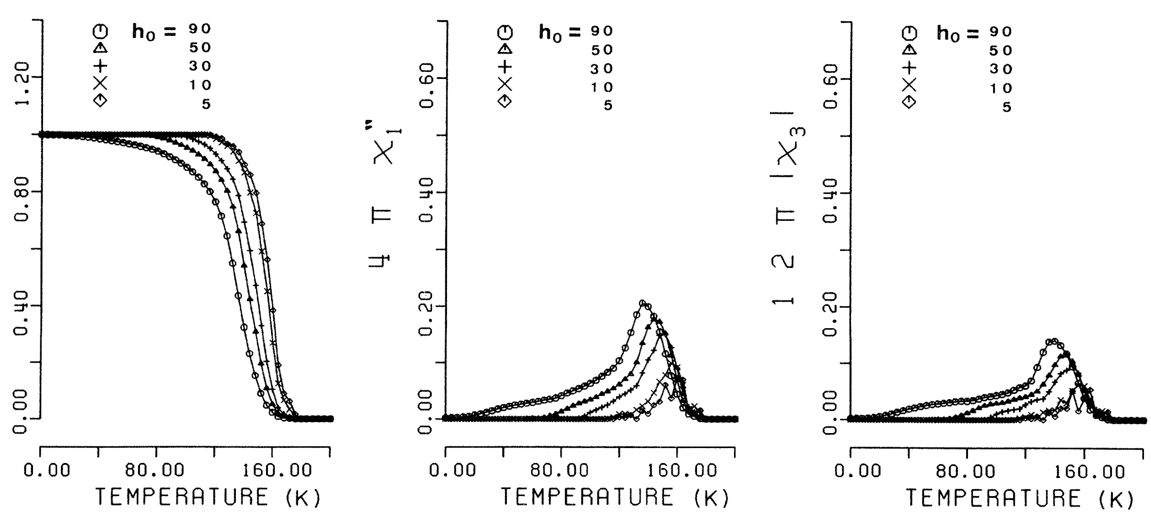


FIG. 10. Simulated results of the fundamental and third-harmonic susceptibility in terms of randomly coupled superconducting chains (Fig. 9). Results reproduce the observations well (Figs. 1 and 3).

becomes difficult to expel the magnetic field by completing a superconducting diamagnetic loop. This effect plausibly leads to the less-prominent Meissner effect and to the smallness of the peak height both in $\chi_1''$ and $|\chi_3|$. The calculation suggests that the peak growth in Figs. 4 and 8 is also related to a disorder in the weak couplings. Although the qualitative explanation can be thus given, it is generally difficult to evaluate the diamagnetic flow pattern in a complicated system. In recent years the fractal approach has been attempted for the diamagnetism of superconducting percolating clusters, but theoretical treatment has thus far been limited to the dc diamagnetic susceptibility.[22–25] Modification of the theory is needed to deal with the present parallel-field case. We hope that the ac measurement would also give a useful probe to examine the recent models.

## ACKNOWLEDGMENTS

Numerical calculation has been performed with the aid of FACOM-M382 computer of the computer center of Kyoto University. One of the authors (T.I.) is indebted to the Japan Society for the Promotion of Science for a grant.

*Present address: Department of Physics, Ibaraki University, Mito, Ibaraki, Japan.

[1]See, for example, Ø. Fischer, Appl. Phys. 16, 1 (1978).
[2]R. L. Greene, G. B. Street, and L. J. Suter, Phys. Rev. Lett. 34, 577 (1975).
[3]Y. Oda, G. Fujii, and H. Nagano, Jpn. J. Appl. Phys. 21, L37 (1982).
[4]T. Ishida and H. Mazaki, in *Proceedings of the International Cryogenic Materials Conference, Kobe, 1982,* edited by K. Tachikawa and A. Clark (Butterworths, London, 1982), p. 430.
[5]See for example, P. Monceau, Physica 109 + 110B, 1890 (1982).
[6]A. F. J. Ruysink, F. Kadijk, A. J. Wagner, and F. Jellinek, Acta Crystallogr. B 24, 1614 (1968).
[7]D. E. Prober, R. E. Schwall, and M. R. Beasley, Phys. Rev. B 21, 2717 (1980).
[8]J. Rosenblatt, Rev. Phys. Appl. 9, 217 (1974).
[9]T. Ishida and H. Mazaki, J. Appl. Phys. 52, 6798 (1981).
[10]T. Ishida and H. Mazaki, Phys. Lett. 87A, 373 (1982).
[11]G. Deutscher, I. Grave, and S. Alexander, Phys. Rev. Lett. 48, 1497 (1982).
[12]K. Selte and A. Kjekshus, Acta Crystallogr. 17, 1568 (1964).
[13]J. G. Smeggil, J. Solid State Chem. 3, 248 (1971).
[14]E. Amberger, K. Polborn, P. Grimm, M. Dietrich, and B. Obst, Solid State Commun. 26, 943 (1978).
[15]Y. Oda, H. Takenaka, H. Nagano, and I. Nakada, Solid State Commun. 32, 659 (1979); 35, 887 (1980).
[16]C. M. Bastuscheck, R. A. Buhrman, and J. C. Scott, Phys. Rev. B 24, 6707 (1981).
[17]T. Ishida, H. Mazaki, and I. Nakada, Proceedings of the International CNRS Colloque, Savoie, 1982, [J. Phys. (Paris) Colloq. C3 44, 1701 (1983)].
[18]Y. Ishihara and I. Nakada, Solid State Commun. 44, 1439 (1982).
[19]T. Ishida, K. Kanoda, and H. Mazaki, Bull. Inst. Chem. Res Kyoto Univ. 61, 45 (1983).
[20]D. L. Martin, Phys. Rev. 141, 576 (1966).
[21]E. Maxwell and M. Strongin, Phys. Rev. Lett. 10, 212 (1963).
[22]P. G. de Gennes, C. R. Acad. Sci. Ser. B 292, 9 (1981); 292, 279 (1981).
[23]M. J. Stephen, Phys. Lett. 87A, 67 (1981).
[24]S. Alexander, Phys. Rev. B 27, 1541 (1983).
[25]R. Rammal, T. C. Lubensky, and G. Toulouse, Phys. Rev. B 27, 2820 (1983).